





## RESEARCH ARTICLE

# Ionization, intrinsic basicity, and intrinsic acidity of unsaturated diols of astrochemical interest: 1,1- and 1,2-ethenediol: A theoretical survey

Otilia Mó<sup>1</sup>  | Al Mokhtar Lamsabhi<sup>1</sup>  | Jean-Claude Guillemin<sup>2</sup>  | Manuel Yáñez<sup>1</sup> 

<sup>1</sup>Departamento de Química, Módulo 13, Facultad de Ciencias, and Institute for Advanced Research in Chemical Sciences (IAdChem), Universidad Autónoma de Madrid, Campus de Excelencia UAM-CSIC, Madrid, Spain

<sup>2</sup>Univ Rennes, Ecole Nationale Supérieure de Chimie de Rennes, CNRS, ISCR- UMR 6226, Rennes, France

## Correspondence

Al Mokhtar Lamsabhi and Manuel Yáñez, Departamento de Química, Módulo 13, Facultad de Ciencias, and Institute for Advanced Research in Chemical Sciences (IAdChem), Universidad Autónoma de Madrid, Campus de Excelencia UAM-CSIC, Cantoblanco, 28049 Madrid, Spain.  
Email: [mokhtar.lamsabhi@uam.es](mailto:mokhtar.lamsabhi@uam.es); [manuel.yanez@uam.es](mailto:manuel.yanez@uam.es)

## Funding information

Comunidad de Madrid; Ministerio de Ciencia, Innovación y Universidades

## Abstract

The structure, stability, and bonding characteristics of 1,1- and 1,2-ethenediol, their radical cations, and their protonated and deprotonated species were investigated using high-level ab initio G4 calculations. The electron density of all the neutral and charged systems investigated was analyzed using the QTAIM, ELF, and NBO approaches. The vertical ionization potential (IP) of the five stable tautomers of 1,2-ethenediol and the two stable tautomers of 1,1-ethenediol go from 11.81 to 12.27 eV, whereas the adiabatic ones go from 11.00 to 11.72 eV. The adiabatic ionization leads to a significant charge delocalization along the O-C-C-O skeleton. The most stable protonated form of (Z)-1,2-ethenediol can be reached by the protonation of both the *anti-anti* and the *syn-anti* conformers, whereas the most stable deprotonated form arises only from the *syn-anti* one. Both charged species are extra-stabilized by the formation of an O-H...O intramolecular hydrogen bond (IHB) which is not found in the neutral system. (Z)-1,2-ethenediol is predicted to be less stable, less basic, and more acidic than its *cis*-glycolaldehyde isomer. The most stable protonated species of (E)-1,2-ethenediol comes from its *syn-syn* conformer, although the *anti-anti* conformer is the most basic one. Contrarily, the three conformers yield a common deprotonated species, so their acidity follows exactly their relative stability. Again, the (E)-1,2-ethenediol is predicted to be less stable, less basic, and more acidic than its *trans*-glycolaldehyde isomer. Neither the neutral nor the protonated or the deprotonated forms of 1,1-ethenediol show the formation of any O-H...O IHB. The most stable protonated species is formed by the protonation of any of the two tautomers, but the most stable deprotonated form arises exclusively from the *syn-anti* neutral conformer. The conformers of 1,1-ethenediol are much less stable and significantly less basic than their isomer, acetic acid, and only slightly more acidic.

Dedicated to Prof. Elfi Kraka on the occasion of her 70th birthday.

This is an open access article under the terms of the [Creative Commons Attribution-NonCommercial-NoDerivs](https://creativecommons.org/licenses/by-nc-nd/4.0/) License, which permits use and distribution in any medium, provided the original work is properly cited, the use is non-commercial and no modifications or adaptations are made.

© 2023 The Authors. *Journal of Computational Chemistry* published by Wiley Periodicals LLC.

## KEYWORDS

1,1-ethenediol, 1,2-ethenediol, acidity, basicity, ionization

## 1 | INTRODUCTION

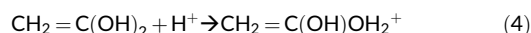
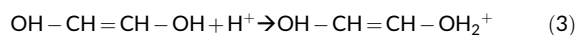
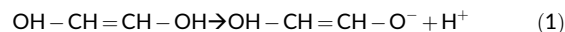
Diols, chemical compounds containing two hydroxyl groups, are ubiquitous in chemistry as they are involved in a huge number of chemical reactions.<sup>1</sup> The aliphatic diols are also known as glycols.<sup>2</sup> Ethylene glycol, the simplest saturated glycol, that is used as antifreeze agent among other industrial applications,<sup>3</sup> has been heavily investigated, because *cis*- and *trans*-ethylene glycol could have played a determining role in prebiotic chemistry. Indeed, many diols and polyols are involved in the mechanism of the formose reaction,<sup>4</sup> a complex autocatalytic set of condensation reactions of formaldehyde, which is a plausible route to prebiotic sugar synthesis, for which some heterogenous routes were proposed.<sup>5</sup> This prebiotic characteristic was also one of the reasons behind the astrochemical interest on this compound, together with the fact that it was, for a long time, one of the largest molecules detected in the interstellar medium.<sup>6,7</sup> Its intramolecular hydrogen bond was investigated by means of *ab initio* calculations,<sup>8</sup> through the use of conventional absorption spectroscopy and laser photoacoustic spectroscopy,<sup>9</sup> and by a theoretical simulation of this spectrum.<sup>10</sup> Also, several theoretical models have been proposed to explain its formation.<sup>11,12</sup> The situation changes completely when moving to the unsaturated diols with a C=C double bond. The first term of the series, the ethenediol, is an elusive compound. The synthesis and characterization by NMR spectroscopy of the 1,2-isomer was reported in 1982,<sup>13</sup> but it was experimentally identified only 2 years ago<sup>14</sup> in low-temperature ices at temperatures of 5 K. The experiments, using photoionization coupled with reflectron time-of-flight mass spectrometry,<sup>14</sup> permit to show its kinetic stability and its potential detectability under interstellar conditions. In the same paper, the structure and relative stabilities of the five conformers of 1,2-ethenediol obtained at the AE-CCSD(T)/cc-PWCVTZ were also given, being in very good agreement with the G4 ones reported in this paper. More recently, the first characterization of the (Z)-1,2-ethenediol by means of rotational spectroscopy was also published.<sup>15</sup> This work led to its detection in the interstellar medium.<sup>16</sup> These two publications deal exclusively with (Z)-1,2-ethenediol, but in ref. 15 equilibrium rotational constants obtained using the CCSD(T)/CBS + CV composite scheme were also provided, being in very good agreement with the corresponding G4-values reported here (see Table S1). This year the photorearrangement of *cis*- and *trans*-1,2-ethenediol to glycolaldehyde has been reported.<sup>17</sup> On the other hand, the 1,1-ethenediol, the enol tautomer of acetic acid, was obtained by decarboxylation of malonic acid for the first time by Mardukov et al.<sup>18</sup> on 2020, and characterized through its IR spectrum by comparing the observed bands with those computed at AE-CCSD(T)/cc-pCVTZ level of theory.<sup>18</sup> 2 years later, it was reported the first bottom-up synthesis of this compound from carbon dioxide and methane.<sup>19</sup>

As mentioned in a recent publication to commemorate the 10 Years of the ACS PHYS Astrochemistry Subdivision,<sup>20</sup> “Astrochemistry is typically thought of as an interdependent triangle consisting of observation, modeling, and laboratory/theoretical insights.” The role of theoretical

simulations in this discipline results obvious in some of the previous paragraphs of this introduction, being particularly useful when dealing with elusive compounds. It would be impossible to summarize the huge number of theoretical studies in the realm of astrochemistry, even if we decide to reduce this survey to the articles published last year, the number would be too high to be included in this introduction. Nevertheless, we have made a very short selection of them to illustrate only a few of the topics in which theoretical analysis may be of particular relevance.<sup>21–30</sup>

In this context, having precise information on the intrinsic reactivity of the elusive unsaturated diols considered in this work might be of importance. This moved us to investigate, through the use of high-level *ab initio* calculations, their ionization, intrinsic basicity, and intrinsic acidity. Indeed, cosmic rays<sup>31</sup> together with X-rays<sup>32,33</sup> and other radiations<sup>34</sup> are responsible for the ionization of many astrochemical species in different regions of cosmos and, in particular, inside molecular clouds.<sup>31</sup> Protonation of these species takes also place in space by reaction with H<sub>3</sub><sup>+</sup>, very abundant in that environment, and this process is of a fundamental importance mainly when dealing with compounds without permanent dipole moment, that otherwise could not be detected by radioastronomy.<sup>35</sup> In particular, that could be the way to detect (E)-1,2-ethenediol in its protonated form. Thus, the formation of protonated or deprotonated species is still of relevance in this context.

In this article, acidities and basicities are calculated as the enthalpy of reactions (1) to (4), at a temperature of 298.150 Kelvin and a pressure of 1.0 Atm.



As indicated in reaction (1), the acidity is the energy required to deprotonate the neutral compound; the larger the value of the enthalpy of reaction (1), the smaller the acidity. The basicity is usually given as the negative of enthalpy of reaction (2) (normally called proton affinity, PA) to use positive values. Both properties can be also measured by using free energies (normally call gas-phase basicity in the case of protonation) but we can anticipate that the conclusions obtained when enthalpies are used, do not change when free energies are employed, since, as shown in Figure S1 of the Supporting Information, for both acidities and basicities, the correlation between enthalpies and free energies for reactions (1)–(4) is very good with excellent linear correlations.

In the low-temperature conditions of interstellar clouds, a description of the stability using electronic energies (including zero-point energy (ZPE) corrections) rather than enthalpies would be

probably preferable. However, as illustrated in Figure S2 of the supporting information, there are no significant differences whatsoever in the stabilities obtained using enthalpies or  $E + \text{ZPE}$  values, since the linear correlations between both sets of values have a slope of 1.006 with a regression coefficient of 0.997.

## 2 | COMPUTATIONAL DETAILS

In order to make a reliable prediction of the intrinsic basicity and acidity of these compounds, it is unavoidable to use an accurate-enough theoretical model. For this purpose, we have decided to use the Gaussian-4 (G4) theory,<sup>36</sup> known to provide energetic outcomes for different thermodynamic properties, for a large set of chemical compounds, with an average absolute deviation ( $3.47 \text{ kJ mol}^{-1}$ )<sup>36</sup> smaller than  $1 \text{ kcal mol}^{-1}$ . This is particularly the case when dealing with intrinsic basicities and acidities,<sup>37,38</sup> even when they are affected by subtle effects induced by weak non-covalent interactions,<sup>39</sup> or when potential astrochemical compounds are involved.<sup>40</sup>

The G4 theory is a composite method based on a balanced combination of well-defined MP2, MP4, and CCSD(T) molecular orbital calculations, where final energies are accurate up to a CCSD(T,full)/G3LargeXP +  $\text{HF}_{\text{limit}}$  level, based on B3LYP/6-31G(2df,p) optimized geometries. The corresponding thermal corrections are also obtained at this DFT level of theory.<sup>36</sup> The reliability of this approach for the study of these kind of systems has been confirmed in ref. 21, by excellent agreement between the experimental acidities and basicities of a suitable set of compounds<sup>41–43</sup> with the G4 calculated outcomes.

The bonding characteristics of the diols under scrutiny were analyzed using three complementary procedures, namely the atoms in molecules (AIM) theory,<sup>44</sup> the natural bond orbital (NBO) method,<sup>45</sup> and the electron localization function (ELF) formalism.<sup>46</sup> The AIM describes the topology of the molecular electron density,  $\rho(r)$ , by locating its critical points associated with the nuclei (maxima), bond critical points (BCPs) (first-order saddle points located between two maxima) which indicate the existence of a chemical linkage, whose nature is associated with the value and sign of the Laplacian of the density,  $\nabla^2\rho(r)$ , and ring critical points (RCPs) (second-order saddle points associated with the formation of a cyclic structure). This information can be also visualized by means of the so-called molecular graphs formed by the lines (bond paths) connecting neighbor maxima and containing a BCP. All these calculations have been carried out by using the AIMAll (Version 19.10.12) code.<sup>47</sup>

The NBO method<sup>45</sup> is based on the use of localized hybrid orbitals and lone pairs obtained as local block eigenvectors of the one-particle density. The bonding patterns stabilizing the system are well described by the characteristics of these hybrid orbitals and a second-order perturbation formalism permits also to evaluate the interaction energies between occupied and empty orbitals.

The ELF approach permits to define the areas in which the electrons of the system are distributed and that can be classified in monosynaptic (associated with core electrons and/or lone pairs), disynaptic (associated with normal chemical bonds), or polysynaptic (for multiple center bonds) basins.

## 3 | RESULTS AND DISCUSSION

In agreement with recent theoretical calculations,<sup>19</sup> five different conformers have been found to be stable in our G4 survey for 1,2-ethenediol, the (Z) arrangement with two different conformers *syn-anti* and *anti-anti* and the (E) arrangement with three conformers, *syn-syn*, *syn-anti*, and *anti-anti* (see Figure 1).

It is worth noting that the (Z) (*anti-anti*) conformer is significantly less stable than the *syn-anti*, which is the global minimum. In these kinds of systems, this is usually assigned to the existence of an intramolecular hydrogen bond (IHB) in the latter. However, in the AIM analysis no BCP is found between the OH and the O atom. This is also in agreement with the NBO analysis that shows a Wiberg bond index<sup>48</sup> for this interaction practically zero (0.01). The favorable *syn-anti* arrangement is clearly associated to a favorable electrostatic interaction between the negatively charged O atom (natural charge  $-0.74$ ) and the positively charged bridging hydrogen atom (natural charge  $+0.50$ ).

The situation is different as far as the (E) conformers are concerned. The enthalpy differences are rather small, so although the *syn-syn* is predicted to be the most stable, the three conformers are practically degenerate within the accuracy of our theoretical model. Actually, in terms of the free energy, the *anti-anti* conformer is the one that is predicted as the global minimum.

For the 1,1-ethenediol two different conformations have been found to be stable (see Figure 1) being the *syn-anti* the global minimum. Again, the enhanced stability of this conformer is essentially of electrostatic nature, since according to the AIM analysis no IHB is formed. The NBO analysis shows similar natural charges for the O and H atoms involved in the interactions as the ones reported above for the (Z)-1,2-ethenediol (*syn-anti*).

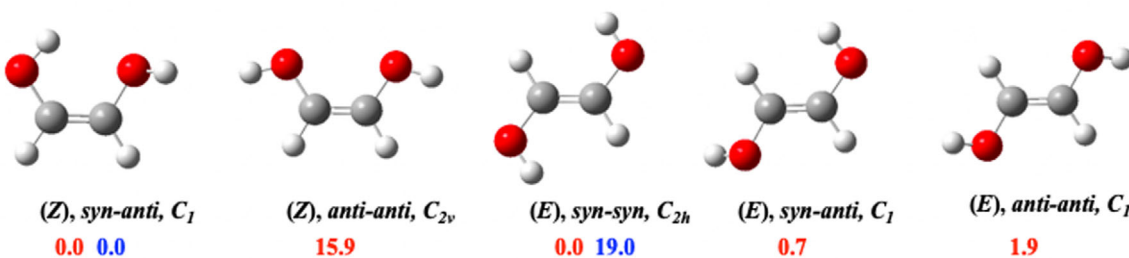
## 4 | IONIZATION

In Table 1, we show the vertical and the adiabatic ionization potential (IP) of the different species under scrutiny.

Due to the absence of experimental information for these unsaturated diols, a suitable reference can be the corresponding saturated counterpart, ethylene glycol. In all cases the vertical IPs for both the 1,2- and the 1,1-ethenediols, in their different conformations, are significantly larger than that of ethylene glycol ( $10.55 \text{ eV}$ ),<sup>49</sup> very likely due to the effect that the IHB in the saturated diol has on its IP.<sup>50</sup>

In order to analyze the ionization effects on the structures of these unsaturated diols we are going, for the sake of simplicity, to focus our attention on the three global minimum of each family, since similar effects are found for all the other conformers. The observed general feature is a significant change in the internuclear distances within the O-C-C-O skeleton, where the C=C bond lengthens in average  $0.07 \text{ \AA}$ , whereas the C-O bonds shorten on average  $0.08 \text{ \AA}$ . Concomitantly, both OH groups lie on the molecular plane, so, for instance, whereas the neutral form of the (Z)-1,2-ethenediol has  $C_1$  symmetry because the *anti*-OH does not lie in the molecular plane, the corresponding radical cation has Cs symmetry.

## 1,2-ethenediol



## 1,1-ethenediol

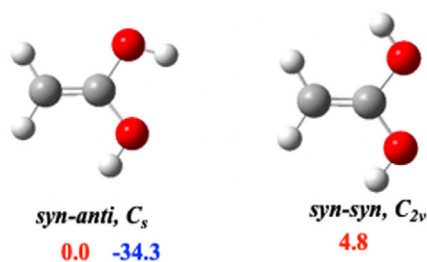


**FIGURE 1** Five conformers, belonging to the two subfamilies, (Z) and (E), of 1,2-ethenediol, and the two of 1,1-ethenediol are shown. Relative enthalpies are given in  $\text{kJ}\cdot\text{mol}^{-1}$ . In blue we show the relative enthalpy of the (E) *syn-syn* and the *syn-anti* 1,1-ethenediol global minima with respect to the (Z) *syn-anti* one.

**TABLE 1** Vertical and adiabatic ionization potential for 1,2-ethenediol and 1,1-ethenediol. All values in eV.

Compound	Vertical IP	Adiabatic IP
(Z)-1,2-ethenediol		
<i>syn-anti</i>	12.12	11.31
<i>anti-anti</i>	11.85	11.08
(E)-1,2-ethenediol		
<i>syn-syn</i>	11.89	11.36
<i>syn-anti</i>	12.07	11.20
<i>anti-anti</i>	11.81	11.00
1,1-ethenediol		
<i>syn-anti</i>	12.17	11.58
<i>syn-syn</i>	12.25	11.72

This can be understood taking into account that the HOMO of all the investigated diols is the C-C  $\pi$  orbital. Hence, when the diol is ionized the electron is removed from this orbital, what results in a reduction in the C-C bond order, from a typical double bond in the neutral to an intermediate situation between a single and a double bond. At the same time, this depopulation enhances the electronegativity of both carbon atoms that polarize the O lone pairs, which indicates that a significant charge delocalization is taking place. Such a delocalization results evident when the molecular graphs of the neutrals are compared with their respective radical cations, showing a clear decrease of the electron density at the C=C BCP, and a parallel increase at the two C-O BCPs (see Figure 2). Consistently, the ELF analysis shows that in all cases, upon ionization, the C-C basin becomes depopulated

with one electron less than in the neutral, whereas the population of both C-O basins increases 0.4 e on average. Finally, the picture provided by the NBO method ratifies the AIM and ELF descriptions. Taking the global minimum of the (Z)-1,2-ethenediol as a suitable example, the Wiberg bond order of the C=C bond decreases from 1.82 in the neutral to 1.29 in the radical cation, but at the same time this indicator increases for the C-O bonds from 0.96 and 0.91, in the neutral to 1.29 and 1.22, respectively, in the radical cation. In summary, the different electron density analyses show that ionization is followed in all cases by a significant charge delocalization as shown in Scheme 1 due to the nature of the HOMO of the neutral diols.

## 5 | PROTONATION AND DEPROTONATION

### 5.1 | (Z)-1,2-ethenediol tautomers

We will start our discussion of the protonation and deprotonation process with the (Z)-1,2-ethenediol tautomers. The results obtained for both processes have been summarized in Figure 3.

Three different conformations have been found to be stable for the protonated forms of (Z)-1,2-ethenediol. As illustrated in Figure 3 the most stable one, of  $C_1$  symmetry, can be reached both by protonation of the most stable *syn-anti* conformer of (Z)-1,2-ethenediol and by the protonation of the *anti-anti* conformer. This indicates that the *anti*-OH group of the neutral global minimum is more basic than the *syn*-OH group. Also interestingly, the most stable protonated form is stabilized by the formation of an IHB, not observed in the neutral. This

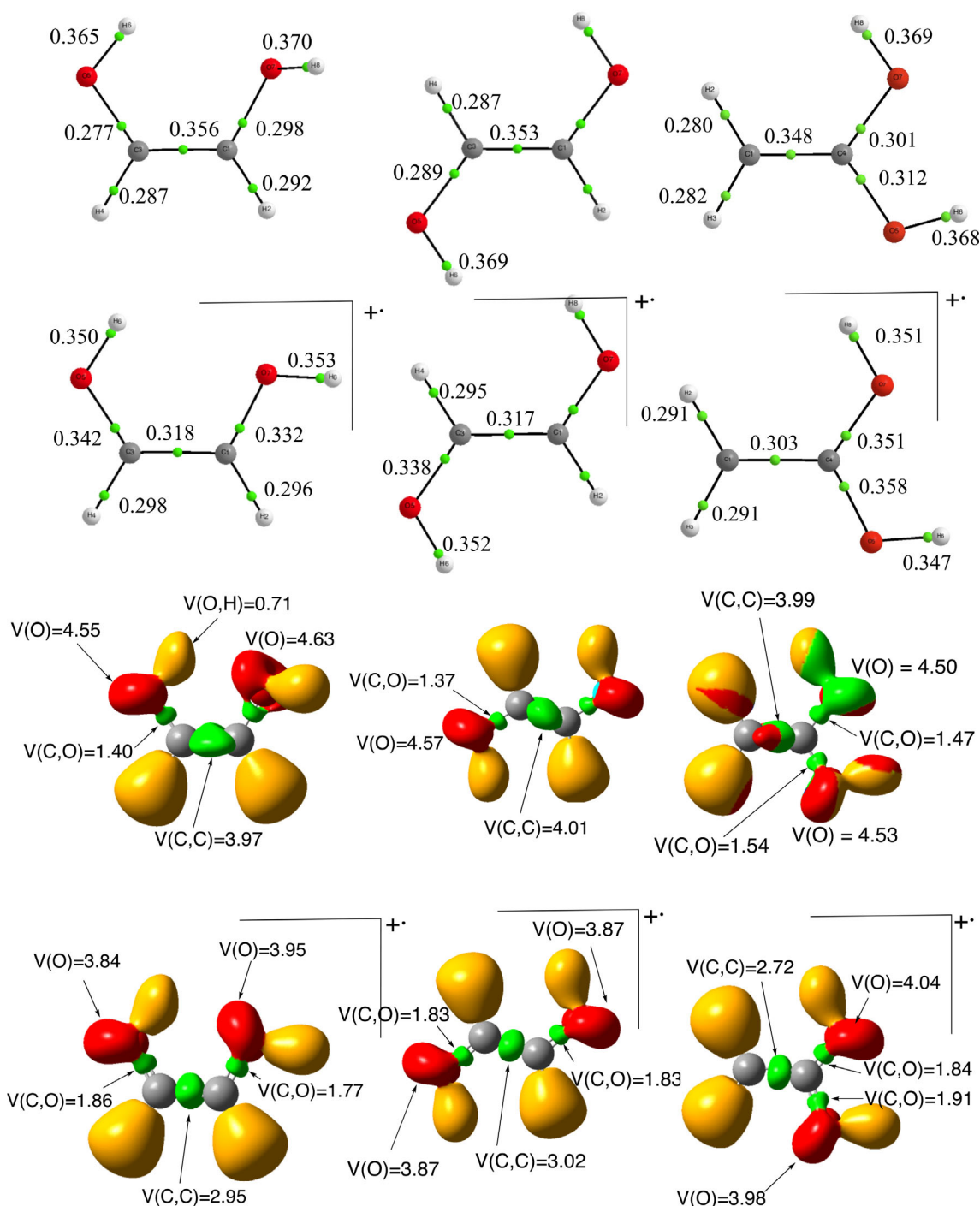


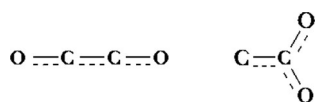
**FIGURE 2** Molecular graphs (first two lines) and ELF plots (last two lines) for the neutral and radical cation species for the most stable conformers of (Z)- and (E)-1,2-ethenediol and 1,1-ethenediol. Electron densities in a.u. and the population basins in e.

is evident when looking at the corresponding molecular graph, that shows the existence of a BCP in the OH...O region, and by the fact that the electron density at the O-H group acting as the proton donor (0.334 a.u.) is clearly smaller than that of the O-H acting as proton acceptor (0.361 a.u.; see left part of Figure 4). The ELF analysis also shows evidences of the formation of this IHB by the decrease of the population at the lone pair of the OH group acting as proton acceptor (from 4.75 to 4.42) and by a significant population at the OH group

acting as the proton donor (from 1.76 to 1.89), which is coherent with the NBO second-order perturbation analysis showing a non-negligible interaction ( $8 \text{ kJ mol}^{-1}$ ) OH...O. All these changes are related with the fact that the protonation of (Z)-1,2-ethenediol takes place at the syn-OH group of the neutral. This implies a substantial charge transfer from this oxygen atom to the incoming proton and, as an obvious consequence, the syn-OH group becomes a much better proton donor than in the neutral favoring the formation of the IHB. It is worth

mention that the two OH groups involved in the IHB are almost coplanar, the dihedral OH...OH angle being  $164.4^\circ$ , whereas in the neutral compound the same dihedral angle is  $109.5^\circ$ .

Two stable tautomers are found upon deprotonation of (Z)-1,2-ethenediol, but in this case the most stable conformer can only be



**SCHEME 1** Delocalization observed upon ionization of 1,2- and 1,1-ethenediols.

directly reached from the most stable *syn-anti* neutral. As it was the case for the protonated species the most stable anionic form is extra-stabilized by a IHB (see right part of Figure 4). In this case, the most stable anion comes from the deprotonation of the *anti*-OH group, with the consequence that the O atom becomes a much better proton acceptor (note that the population of the oxygen basins increase from 4.42 e in the neutral to 5.91 e in the anion), favoring the formation of the IHB.

Finally, it should be mentioned that, with respect to the diol, its *cis*-glycolaldehyde (hydroxyacetaldehyde) isomer is predicted to be  $33 \text{ kJ}\cdot\text{mol}^{-1}$  more stable, more basic (proton affinity (PA)  $782.9 \text{ kJ}\cdot\text{mol}^{-1}$  vs.  $754.0 \text{ kJ}\cdot\text{mol}^{-1}$ ), and significantly less acidic

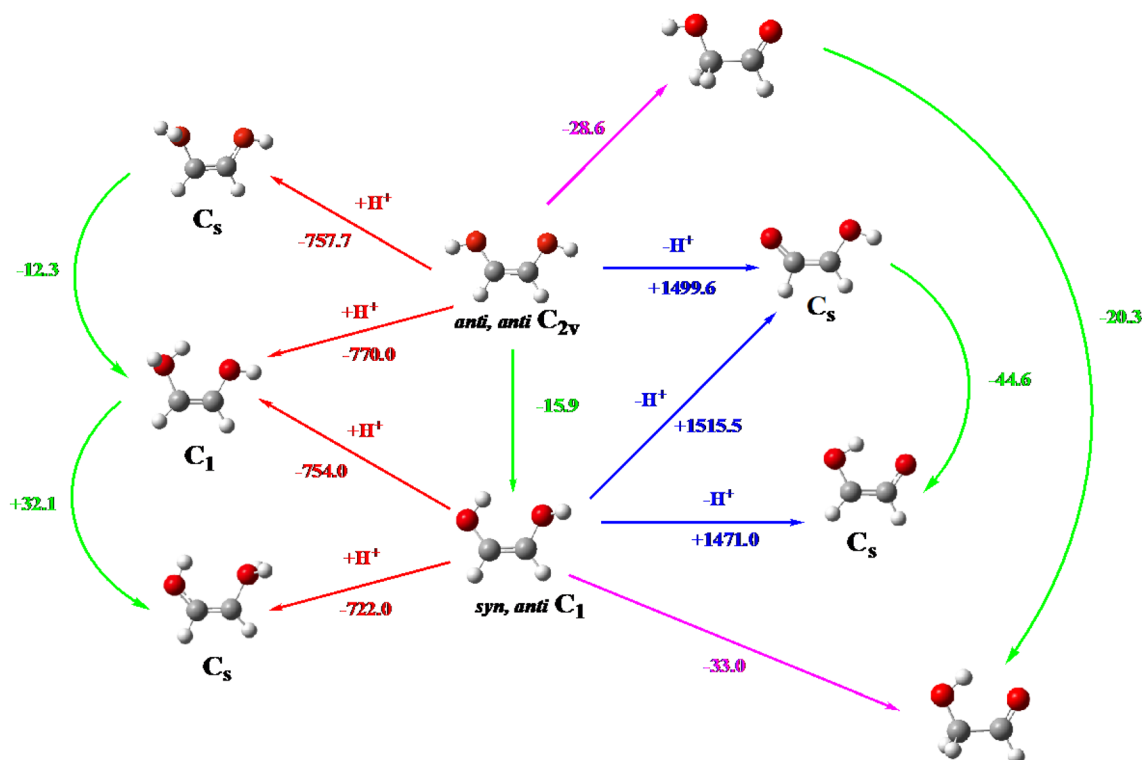


**FIGURE 3** Scheme showing the protonation (red arrows) and the deprotonation (blue arrows) of the two conformers of (Z)-1,2-ethenediol. Magenta arrows correspond to the processes to yield the corresponding conformers of its isomer *cis*-glycolaldehyde. Green arrows provide information on the relative stability of different species. All values are in  $\text{kJ}\cdot\text{mol}^{-1}$ .

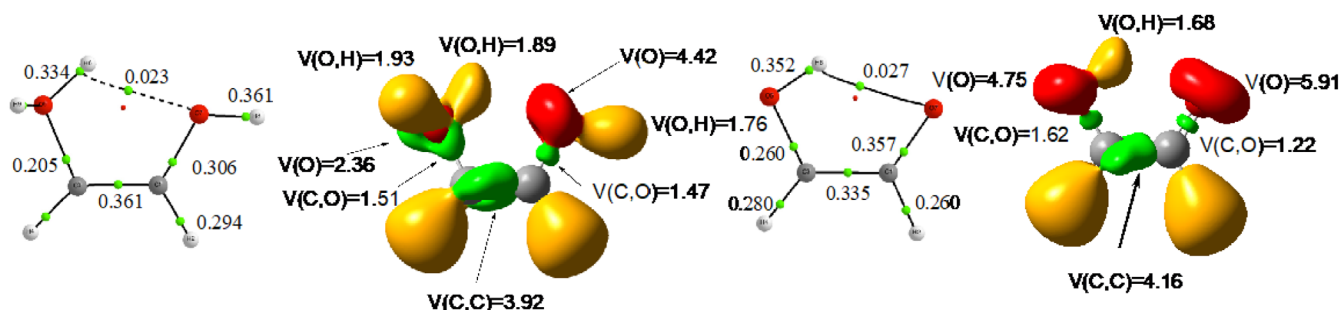


**FIGURE 4** Molecular graphs and ELF plots for the most stable protonated and deprotonated forms of (Z)-1,2-ethenediol. Electron densities in a.u. and the population basins in e.



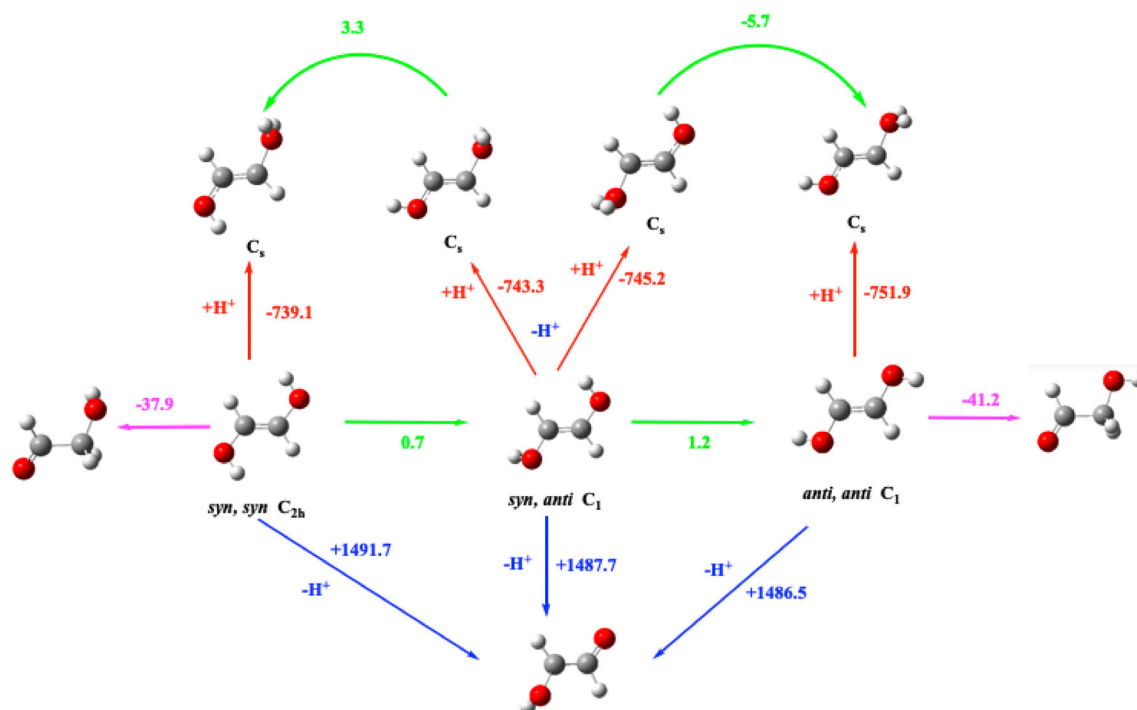


**FIGURE 5** Scheme showing the protonation (red arrows) and the deprotonation (blue arrows) of the three conformers of (*E*)-1,2-ethenediol. Magenta arrows correspond to the processes to yield the corresponding conformers of its isomer *trans*-glycolaldehyde. Green arrows provide information on the relative stability of different species. All values in kJ·mol<sup>-1</sup>.

(1538.8 kJ·mol<sup>-1</sup> vs. 1471.0 kJ·mol<sup>-1</sup>, see Figure 3). The experimental basicity of glycolaldehyde has not been measured but our calculated value for its acidity is in very good agreement with the experimental one (1536 ± 8.4 kJ·mol<sup>-1</sup>).<sup>51</sup>

## 5.2 | (*E*)-1,2-ethenediol tautomers

The energetic data (in terms of enthalpies) corresponding to the protonation and deprotonation processes of the (*E*)-1,2-ethenediol tautomers are shown in the scheme of Figure 5.

As expected, due to their symmetry, the *syn-syn* and the *anti-anti* conformers yield a unique protonation tautomer each, whereas the protonation of the non-symmetric *syn-anti* conformer leads to two different protonated species since both hydroxyl groups are not equivalent. The PAs obtained indicate that the most stable conformer is the less basic one, being the most basic the *anti-anti* conformer. Quite unexpectedly, the deprotonation of the three conformers lead to a common anion of  $C_1$  symmetry because, in all cases, the most stable anion corresponds to a structure in which the remaining OH group undergoes a torsion that puts it perpendicular to the plane of the rest of the molecule, where the character *syn* or *anti* disappears. Nevertheless, a  $C_s$  minimum in which this OH group remains in the plane of the molecule and in position *syn*, also exists (see Figure S3), but it is 3.2 kJ mol<sup>-1</sup> higher in energy. The obvious consequence is that the intrinsic acidity of the three *E*-conformers follows the inverse sequence to their stability, being the most acidic one the *anti-anti*

conformer. Interestingly, as shown in Figure 5, this tautomer is also the most basic one.

It can be also observed that these *E*-diols are less stable than the corresponding *trans*-glycolaldehyde tautomers and slightly less basic (diol PA = 751.9 vs. *trans*-glycolaldehyde PA = 758.4 kJ mol<sup>-1</sup>). All diol tautomers are, however, more acidic than *trans*-glycolaldehyde, whose acidity, at the same level of theory, is 1521.5 kJ mol<sup>-1</sup>.

## 5.3 | 1,1-ethenediol tautomers

As indicated above, two stable conformers have been located for 1,1-ethenediol, both been rather close in energy. Although the global minimum presents two non-equivalent hydroxyl groups, the protonation at the *anti*-OH leads to the same protonated species obtained when the proton attachment takes place at the *syn*-OH, because in this latter case the attached proton is spontaneously shifted to the other hydroxyl group. The obvious consequence is that the less stable conformer is the more basic one (see Figure 6).

As we discussed above the *syn-anti* neutral conformer does not exhibit the formation of any IHB, what is reflected in the small energy gap with respect to the *syn-syn* one. However, in this case and contrarily to what was observed for (*Z*)-1,2-ethenediol, the protonated form does not exhibit any IHB either as reflected in the corresponding molecular graph (see Figure 7). It can be observed that protonation at the *anti*-OH group implies a significant charge depletion from the corresponding C-OH bond, whose electron density at the BCP decreases

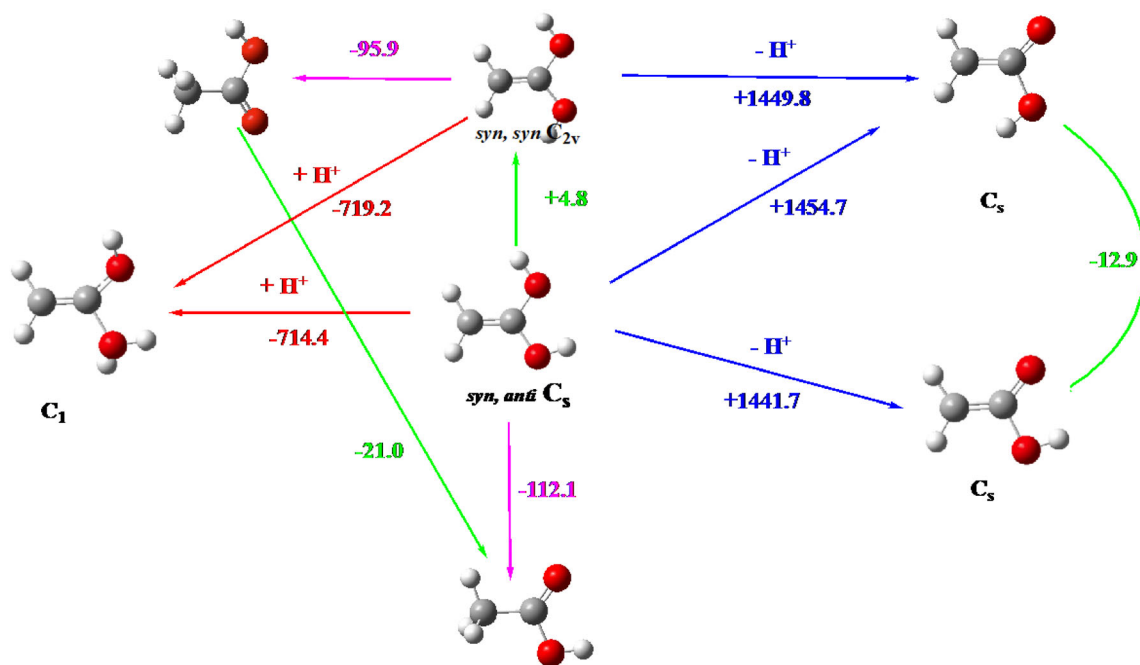


**FIGURE 6** Scheme showing the protonation (red arrows) and the deprotonation (blue arrows) of the two conformers of 1,1-ethenediol. Magenta arrows correspond to the processes to yield the corresponding conformers of its isomer acetic acid. Green arrows provide information on the relative stability of different species. All values in  $\text{kJ}\cdot\text{mol}^{-1}$ .

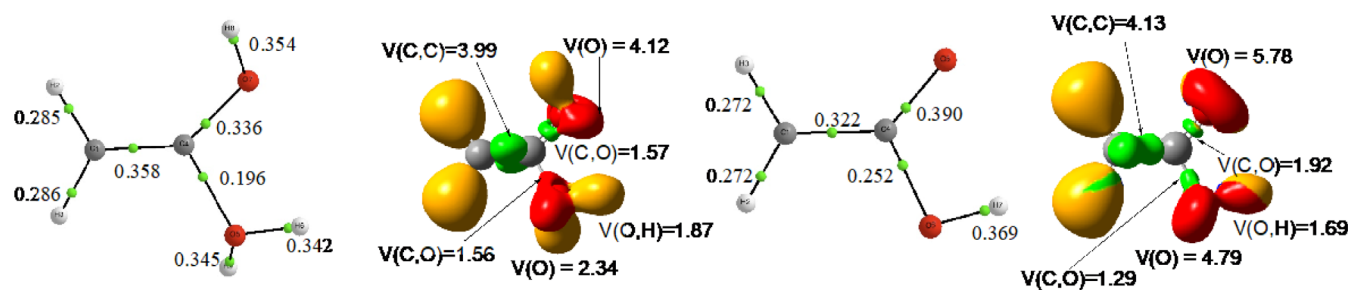


**FIGURE 7** Molecular graphs and ELF plots for the most stable protonated and deprotonated forms of 1,1-ethenediol. Electron densities in a.u. and the population basins in e.

from 0.358 a.u. in the neutral (see Figure 2) to almost half this value in the protonated form (0.196 a.u., see left part of Figure 7). The obvious consequence is an elongation of the C-OH bond by 0.16 Å, what is reflected in a longer OH...O distance (0.1 Å) that renders the possibility of forming a IHB in the protonated cation even smaller than in the neutral. This is ratified by the characteristics of the ELF plots.

As far as the deprotonation is concerned, as shown in Figure 6, the deprotonation of *anti*-OH group of the global minimum (*syn-anti* tautomer) leads to the same anion as the deprotonation of the *syn-syn* tautomer. This anion is almost 13  $\text{kJ}\cdot\text{mol}^{-1}$  less stable than the one generated by deprotonation of the *syn*-OH group of the global minimum. Once again, however, no IHB is found for this species (see right part of Figure 7), although in this case the OH...O distance does not change significantly with respect to the neutral, but as shown by the ELF plot, due to the rigidity imposed by the C=C double bond, the orientation of the OH basin with respect to the O lone pairs is not too favorable to form a

IHB. Indeed, as shown by the ELF plot, although the basin of the oxygen lone pair and the O-H basin are coplanar, they are about parallel to each other rendering very difficult their interaction. Finally, it should be noted that both diols are much less stable and significantly less basic than their isomer, acetic acid (714 and 719  $\text{kJ}\cdot\text{mol}^{-1}$  vs. 788.6  $\text{kJ}\cdot\text{mol}^{-1}$  (calculated); 783.7  $\text{kJ}\cdot\text{mol}^{-1}$  (experimental)<sup>41</sup>), whereas the most stable diol is predicted to be a slightly stronger acid than acetic acid (1441.7  $\text{kJ}\cdot\text{mol}^{-1}$  vs. 1449.0  $\text{kJ}\cdot\text{mol}^{-1}$  (calculated); 1457.  $\pm$  5.9 (experimental)<sup>52</sup>).

## 6 | CONCLUDING REMARKS

The HOMO of all the diols investigated corresponds to the C-C  $\pi$  bond, and as a consequence the ionization of these systems results in a significant charge delocalization along the O-C-C-O for the 1,2-ethenediols and the C-CO<sub>2</sub> skeleton for the 1,1-isomers. In some



cases, the protonation or the deprotonation of different neutral conformers leads to a common cation and/or anion. This is the case, for instance, as far as the protonation of (Z)-1,2-ethenediol is concerned, since its most stable protonated form is reached both by the protonation of both the *anti-anti* and by the protonation of the *syn-anti* conformers. Conversely, the most stable deprotonated form arises only from the *syn-anti* conformer. Very importantly, cation and anion are extra-stabilized by the formation of an O-H...O intramolecular hydrogen bond (IHB) not found in the neutral form from which they proceed. (Z)-1,2-ethenediol is predicted to be less stable, less basic, and more acidic than its *cis*-glycolaldehyde isomer. The most stable protonated species of (E)-1,2-ethenediol comes from its *syn-syn* conformer, but the protonated formed produced is not the most stable one that is the one coming from the *anti-anti* conformer. Contrarily, the three conformers yield a common deprotonated species, so their acidity follows exactly their relative stability. Again, the (E)-1,2-ethenediol is predicted to be less stable, less basic, and more acidic than its *trans*-glycolaldehyde isomer. Neither the neutral nor the protonated or deprotonated 1,1-ethenediol show the formation of any O-H...O IHB due to the rigidity of the molecular framework, that forces the O-H group to be in a position where its effective interaction with the oxygen lone pair is impeded. The most stable protonated form of 1,1-ethenediol arises from the protonation of any of the two tautomers, but the most stable deprotonated form arises exclusively from the *syn-anti* neutral conformer. The conformers of 1,1-ethenediol are much less stable and significantly less basic than their isomer, acetic acid, and only slightly more acidic.

## ACKNOWLEDGMENTS

This work was carried out with financial support from the projects PID2021-125207NB-C31 and PID2019-110091GB-I00 of the Ministerio de Ciencia, Innovación y Universidades of Spain (MICINN) and the project Y2020/EMT-6290 (PRIES-CM) of the Comunidad de Madrid. Finally, the authors thank the Centro de Computación Científica of the UAM (CCC-UAM) for the generous allocation of computer time and continued technical support. J.-C.G. thanks the CNES for a grant.

## DATA AVAILABILITY STATEMENT

The data that support the findings of this study are available from the corresponding author upon reasonable request.

## ORCID

Otilia Mó  <https://orcid.org/0000-0003-2596-5987>

Al Mokhtar Lamsabhi  <https://orcid.org/0000-0002-1509-2513>

Jean-Claude Guillemin  <https://orcid.org/0000-0002-2929-057X>

Manuel Yáñez  <https://orcid.org/0000-0003-0854-585X>

## REFERENCES

- [1] F. A. Carey, R. Sundberg, *J. Advanced Organic Chemistry. Part A: structure and Mechanisms*; Springer Science+Business Media, LLC, New York 2007.
- [2] A. D. McNaught, A. Wilkinson, *Compendium of Chemical Terminology*. IUPAC recommendations; International Union of Pure and Applied Chemistry (IUPAC): Zurich (Switzerland). 2019.
- [3] S. Rebsdat, D. Mayer, *Ullmann's Encyclopedia of Industrial Chemistry* (Ed: C. Ley), Wiley-VCH, Weinheim (Germany) 2006.
- [4] A. Butlerow, *Comp. Rend. Acad. Sci.* **1981**, 53, 145.
- [5] A. H. Weiss, S. Trigerman, G. Dunnells, V. A. Likholobov, E. Biron, *Ind. Eng. Chem. Process Des. Dev.* **1979**, 18(3), 522.
- [6] J. M. Hollis, F. J. Lovas, P. R. Jewell, L. H. Coudert, *Astrophys. J.* **2002**, 571(1), L59.
- [7] V. M. Rivilla, M. T. Beltran, R. Cesaroni, F. Fontani, C. Codella, Q. Zhang, *Astron. & Astrophys.* **2017**, 598, A59.
- [8] R. A. Klein, *J. Comput. Chem.* **2002**, 23(6), 585.
- [9] D. L. Howard, P. Jorgensen, H. G. Kjaergaard, *J. Am. Chem. Soc.* **2005**, 127(48), 17096.
- [10] Y. L. Cheng, H. Y. Chen, K. Takahashi, *J. Phys. Chem. A.* **2011**, 115(22), 5641.
- [11] W. H. Sorrell, *Astrophys. J.* **2001**, 555(2), L129.
- [12] V. Taquet, A. Lopez-Sepulcre, C. Ceccarelli, R. Neri, C. Kahane, S. B. Charnley, *Astrophys. J.* **2015**, 804, 2.
- [13] M.-C. Lasne, J.-L. Ripoll, *Tetrahedron Lett.* **1982**, 23, 1587.
- [14] N. F. Kleimeier, A. K. Eckhardt, R. I. Kaiser, *J. Am. Chem. Soc.* **2021**, 143(34), 14009.
- [15] M. Melosso, L. Bizzocchi, H. Gazzeh, F. Tonolo, J. C. Guillemin, S. Alessandrini, V. M. Rivilla, L. Dore, V. Barone, C. Puzzarini, *Chem. Comm.* **2022**, 58(16), 2750.
- [16] V. M. Rivilla, L. Colzi, I. Jimenez-Serra, J. Martin-Pintado, A. Megias, M. Melosso, L. Bizzocchi, A. Lopez-Gallifa, A. Martinez-Henares, S. Massalkhi, B. Tercero, P. de Vicente, J. C. Guillemin, J. G. de la Concepcion, F. Rico-Villas, S. S. Zeng, S. Martin, M. A. Requena-Torres, F. Tonolo, S. Alessandrini, L. Dore, V. Barone, C. Puzzarini, *Astrophys. J. Lett.* **2022**, 929(1), L11.
- [17] A. Mardiyukov, R. C. Wende, P. R. Schreiner, *Chem. Comm.* **2023**, 59, 2596.
- [18] A. Mardiyukov, A. K. Eckhardt, P. R. Schreiner, *Angew. Chem. Eng. Int. ed.* **2020**, 59(14), 5577.
- [19] N. F. Kleimeier, R. I. Kaiser, *J. Phys. Chem. Lett.* **2022**, 13(1), 229.
- [20] R. C. Fortenberry, R. J. McMahon, R. I. Kaiser, *J. Phys. Chem. A.* **2022**, 126, 6571.
- [21] J. Perrero, J. Enrique-Romero, B. Martínez-Bachs, C. Ceccarelli, N. Balucani, P. Ugliengo, A. Rimola, *ACS Earth Space Chem.* **2022**, 6, 496.
- [22] M. Sanz-Novio, P. Ortega, P. Redondo, A. Largo, J. L. Alonso, C. Barrientos, *Astrophys. J.* **2022**, 941, 40.
- [23] T. Qureshi, S. Løyland, S. J. Jørgensen, E. M. Færgestad, T. Norby, E. Uggerud, *Phys. Chem. Chem. Phys.* **2022**, 24, 15357.
- [24] E. Peña-Asensio, J. M. Trigo-Rodríguez, A. Rimola, *Astron. J.* **2022**, 164, 76.
- [25] M. Simsova-Zamecnikova, P. Soldan, M. Gustafsson, *Astron. & Astrophys.* **2022**, 664, A5.
- [26] I. Baldea, *Adv. Theory Simul.* **2022**, 5, 8.
- [27] K. M. Douglas, D. I. Lucas, C. Walsh, N. A. West, M. A. Blitz, D. E. Heard, *Astrophys. J. Lett.* **2022**, 937, 1.
- [28] K. M. Hickson, J. C. Loison, P. Larregaray, L. Bonnet, V. Wakelam, *J. Phys. Chem. A.* **2022**, 126(6), 940.
- [29] N. Genossar, P. B. Changala, B. Gans, J. C. Loison, S. Hartweg, M. A. Martin-Drumel, G. A. García, J. F. Stanton, B. Ruscic, J. H. Baraban, *J. Am. Chem. Soc.* **2022**, 144, 18518.
- [30] C. N. Shingledecker, T. Banu, Y. Kang, H. J. Wei, J. Wandishin, G. Nobis, V. Jarvis, F. Quinn, G. Quinn, G. Molpeceres, M. C. McCarthy, B. A. McGuire, J. Kaestner, *J. Phys. Chem. A.* **2022**, 126(32), 5343.
- [31] S. Coutu, S. W. Barwick, J. J. Beatty, A. Bhattacharyya, C. R. Bower, C. J. Chaput, G. A. de Nolfo, M. A. DuVernois, A. Labrador, S. P. McKee, D. Muller, J. A. Musser, S. L. Nutter, E. Schneider, S. P. Swordy, G. Tarle, A. D. Tomasch, E. Torbet, *Astrophys. J.* **1999**, 11(4), 429.
- [32] J. H. Krolik, T. R. Kallman, *Astrophys. J.* **1983**, 267(2), 610.
- [33] M. Padovani, D. Galli, A. E. Glassgold, *Astron. & Astrophys.* **2009**, 501(2), 619.

- [34] A. Dalgarno, *Proc. Natl. Acad. Sci.* **2006**, 103(33), 12269.
- [35] S. Alessandrini, L. Bizzocchi, M. Melosso, C. Puzzarini, *Front. Astron. Space Sci.* **2023**, 10, 10.
- [36] L. A. Curtiss, P. C. Redfern, K. Raghavachari, *J. Chem. Phys.* **2007**, 126(8), 84108.
- [37] M. Yáñez, O. Mó, I. Alkorta, J. Elguero, *Chem-Eur. J.* **2013**, 19(35), 11637.
- [38] A. Lamsabhi, M. M. Vallejos, B. Herrera, O. Mó, M. Yáñez, *Theor. Chem. Acc.* **2016**, 135, 6.
- [39] M. M. Montero-Campillo, O. Brea, O. Mó, I. Alkorta, J. Elguero, M. Yáñez, *Phys. Chem. Chem. Phys.* **2019**, 21(5), 2222.
- [40] O. Mó, I. Alkorta, J. C. Guillemin, M. Yáñez, *Theor. Chem. Acc.* **2023**, 142, 3.
- [41] E. P. Hunter, S. G. Lias, *J. Phys. Chem. Ref. Data* **1998**, 27, 413.
- [42] V. F. DeTuri, K. M. Ervin, *J. Phys. Chem. A* **1999**, 103, 6911.
- [43] B. K. Janousek, K. J. Reed, J. I. Brauman, *J. Am. Chem. Soc.* **1980**, 102, 3125.
- [44] R. F. W. Bader, *Atoms in Molecules, A Quantum Theory*; Clarendon Press, Oxford **1990**.
- [45] A. E. Reed, F. Weinhold, *J. Chem. Phys.* **1985**, 83(4), 1736.
- [46] A. Savin, R. Nesper, S. Wengert, T. F. Fassler, *Angew. Chem. Int. Edit.* **1997**, 36(17), 1809.
- [47] T. A. Keith, TK Gristmill Software: Overland Parks KS. **2019**; [aim.tkgristmill.com](http://aim.tkgristmill.com), 2019
- [48] K. B. Wiberg, *Tetrahedron* **1968**, 24(3), 1083.
- [49] K. Kimura, S. Katsumata, Y. Achiba, T. Yamazaki, S. Iwata, *Handbook of HeI Photoelectron Spectra of Fundamental Organic Molecules: Ionization Energies, Ab Initio Assignments, and Valence Electronic Structure for 200 Molecules*, Japan Scientific Soc. Press, Tokyo (Japan) **1981**.
- [50] K. Ohno, K. Imai, Y. Harada, *J. Am. Chem. Soc.* **1985**, 107, 8078.
- [51] J. H. J. Dawson, N. M. M. Nibbering, *Int. J. Mass. Spectrom. Ion. Phys.* **1980**, 33, 3.
- [52] L. A. Angel, K. M. Ervin, *J. Phys. Chem. A* **2006**, 110, 10392.

## SUPPORTING INFORMATION

Additional supporting information can be found online in the Supporting Information section at the end of this article.

**How to cite this article:** O. Mó, A. M. Lamsabhi, J.-C. Guillemin, M. Yáñez, *J. Comput. Chem.* **2023**, 1. <https://doi.org/10.1002/jcc.27223>